COUPLERS FOR CAVITIES

E. Haebel
CERN, Geneva, Switzerland

Abstract

The first part of this chapter is on higher-order-mode couplers. To introduce the subject a coupling approach is examined which makes use of the beam tubes as wave guides with internal vacuum compatible RF loads. Then it is shown how coupling can be considerably enhanced if couplers are themselves regarded as resonators. Examples of couplers used in the LEP and HERA storage rings serve to illustrate this approach. In this first part we regard the cavity as a multi-frequency generator furnishing, via the coupler, power to a room temperature load. In the second part the direction of power flow is reversed. Now, at a single frequency, the cavity acts as a low-temperature load to which RF power has to be delivered and which can be considerably higher than the higher-order-mode power.

1. INTRODUCTION

Cavities are the 'motors' of accelerators, passing energy to the charged particle beams. But charges passing through a cavity are 'active devices' and can either receive energy from, or furnish energy to, a cavity. In an accelerator the first process is the required one though the second inevitably takes place and may hamper the efforts to produce a high quality beam. Couplers are needed to replenish the cavity energy which had been lost to the beam. Such main or power couplers may have to handle very large amounts of RF power, up to the MW level.

Couplers are also needed to mitigate the unwanted interactions between particles and cavities. They then are called *higher-order-mode* (HOM) couplers or dampers. In fact, to be more precise, couplers are RF devices which allow energy to be exchanged with the *modes of oscillation* of a cavity. So, at the beginning of this coupler chapter a short discussion of modes is needed.

2. MODES AND THEIR CLASSIFICATION

The ideal cavity is a closed volume, completely surrounded by a metallic boundary as indicated in Fig. 1. For infinite conductivity of the metal walls a closed volume can store electromagnetic field energy U for infinite time. Storage is in the form of *free oscillations* at eigenfrequencies ω_n, the spectrum of which depends on the size and shape of the volume. At each ω_n, field energy U_n changes periodically between its two possible forms, electric and magnetic, and the patterns of the corresponding fields E_n and H_n are characteristic of each oscillation mode. Computer codes are available (e.g. MAFIA) to calculate the eigenfrequencies and fields of such modes but for simple boundary shapes analytical solutions also exist. Two examples are shown in Fig. 2.

For accelerator cavities it is usual to classify the cavity modes into two groups: the first contains only a single member, the mode used for particle acceleration, the second group contains all the others. Since, by cavity design, the accelerating mode usually has the lowest frequency, one calls it the *fundamental mode* (fm) and all the others the *higher-order modes*. Another name for the latter is *parasitic modes*, indicating that they are deleterious and unwanted. I will also talk about longitudinal and dipole modes. Cavities for accelerators have axial symmetry. Then in a cylindrical coordinate system ϕ, r and z, longitudinal modes have fields with no ϕ dependence whereas for dipole modes fields vary with $\cos\phi$.

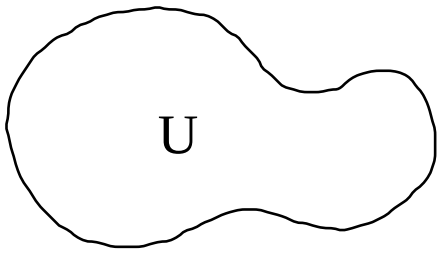

Fig. 1 Example of an ideal cavity

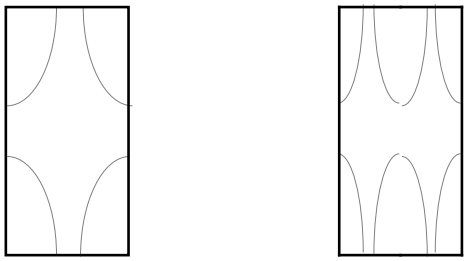

Fig. 2 The TM011- and TM012-mode E-field patterns of a 'pillbox' cavity

3. BEAM TUBES AS HOM DAMPERS

To integrate a cavity into an accelerator one has to attach it to the beam tubes These have little influence on modes with eigenfrequencies lower than the cut off frequency of wave propagation in the beam tubes. Cavity modes with higher frequencies are often said to be *propagating.* It is assumed that, by exciting waveguide travelling-wave modes, such cavity modes will quickly loose their stored energy i.e. become very effectively damped.

The interesting question is now: Can *all* HOM of a cavity be made propagating? What beam tube diameter is required to achieve this goal? To get a first idea we do some back of the envelope calculations. They become simple if the cavity has the shape of a pillbox with radius *a* and length *l*. For this simple shape the fundamental TM_{010} resonance is at the cut off frequency of the TM_{01} waveguide mode in a tube of radius *a*. This mode has the propagation constant:

$$k^2 = \left(2\pi/\Lambda\right)^2 = \left(\omega/c\right)^2 - \left(2.41/a\right)^2$$

At the cut off the propagation constant is zero and hence at the TM_{010} resonance frequency f_0:

$$\omega_0/c = \left(2.41/a\right)$$

Note that f_0 is independent of the pillbox length 1. Cavities for ultra-relativistic particles have lengths around $\lambda_0/2$ where λ_0 is the free space wavelength at f_0. The HOM next to the fundamental then is the TE_{111} dipole mode. At its resonance the cavity length is one half of the TE_{11} mode wavelength. Working again with the propagation constant we can therefore determine its frequency from

$$\left(2\pi/\Lambda\right)^2 = \left(2\pi/2l\right)^2 = \left(\omega_1/c\right)^2 - \left(1.841/a\right)^2$$

The beam tube radius *b,* which at ω_1 just allows propagation of the TE_{11} mode can then be calculated since

$$\omega_1 / c = 1.841 / b \ .$$

Writing finally $l = p\,\lambda_0/2$ and rearranging we obtain for the ratio *a/b* of cavity and beam tube radius:

$$(a/b)^2 = 1 + (1/p)^2 (2.41/1.84)^2$$

To have, according to this formula, propagation of all HOM, the beam tubes must be much wider than conventionally used and a reasonable value of $a/b = 2$ is only obtained if $p = 0.75$ i.e. for a cavity *shorter than* $\lambda_0/2$. This prevents us using such a HOM damping technique for multicell π-mode cavities. Even for a single cell the prognostic from this formula is too optimistic. A check with a code like URMEL reveals [1] that attaching wide beam tubes to the

cell *lowers* its TE_{111} frequency, so the mode 'refuses' to propagate *however wide the beam tubes are made!*

3.1 Confined and trapped modes

Figure 3 shows *E*-field patterns of a wide-beam-tube design [2] as studied at CERN for possible use in LHC. The FM frequency is 400 MHz and the beam tube diameter 30 cm, about one half of the cavity diameter. The TE_{11} and TM_{01} waveguide cut off frequencies are 586 and 764 MHz respectively and, as we see in comparing frequencies, in addition to the FM also the TE_{111} and TM_{110} dipole modes remain *confined* to the cavity. The TM_{011} mode (first harmonic of the fundamental) just reaches the region of propagation. But even a frequency above cut off is no guarantee of sufficient mode damping. At about three times the fundamental mode frequency (at 1232 MHz) we see a HOM which excites only a very small field in the beam tubes. For a cell length of $\lambda_0/2$ the excitation would be even weaker. We have here the example of a *trapped mode* which, though *nominally propagating*, may remain weakly damped [3]. Trapped modes become a real headache when designing multicell cavities [4]. They also have smaller cell-to-cell coupling than other modes so, with increasing cell numbers, field distributions become very sensitive to perturbations.

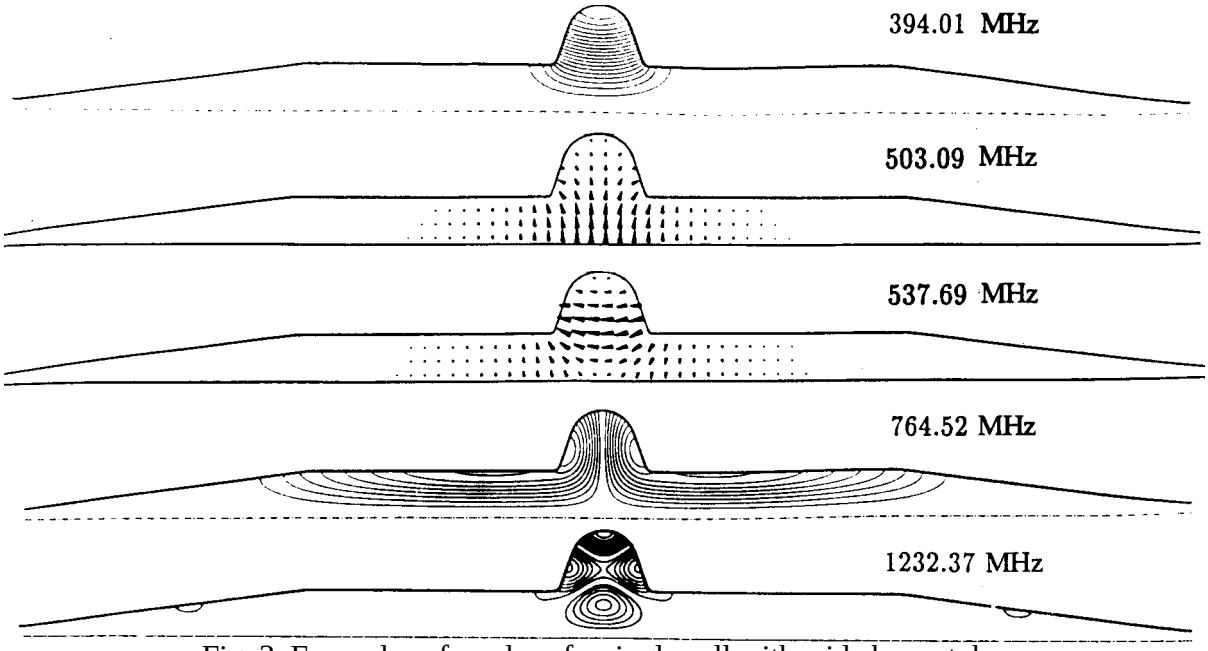

Fig. 3 Examples of modes of a single cell with wide beam tubes

3.2 Deconfining the TE_{111} mode

To escape from the dilemma of the first two dipole modes not propagating, two solutions were proposed and developed. The first, as pursued at KEK in Japan, simply widens the beam tube further, but only behind a coupling aperture to the cell[1] as sketched in Fig. 4. However, not only the TE_{11} cut off is lowered but also, unnecessarily, the TM_{01} cut off, so at the RF absorbing material the FM amplitude might become too high. Therefore, at Cornell the beam tube is widened azimuthally only in sectors, which creates the geometry of a ridged waveguide (see Fig. 4) and lowers particularly the waveguide's dipole mode cut off. These techniques are used for one of the beam tubes, the other tube (see Fig. 5) remaining a simple one. The use of

[1] This concept was already applied by the Wuppertal team in their designs of 3-GHz structures.

different beam tube sections on the two sides of the single cell helps to avoid trapped modes, measurements on a copper model at Cornell demonstrating efficient damping of all significant modes to external *Q* values smaller than 50.

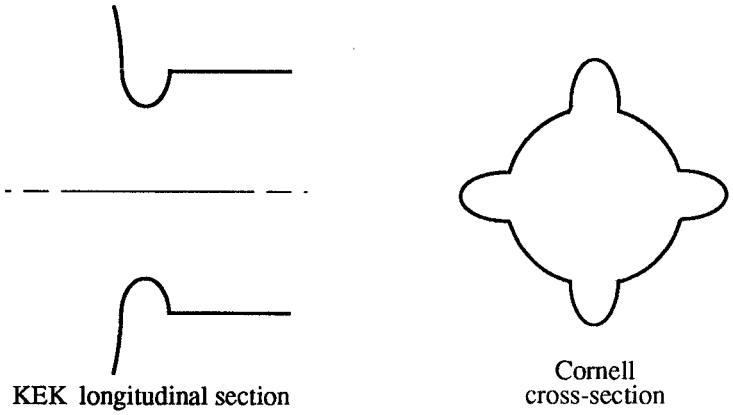

Fig. 4 Beam tube forms at KEK and Cornell

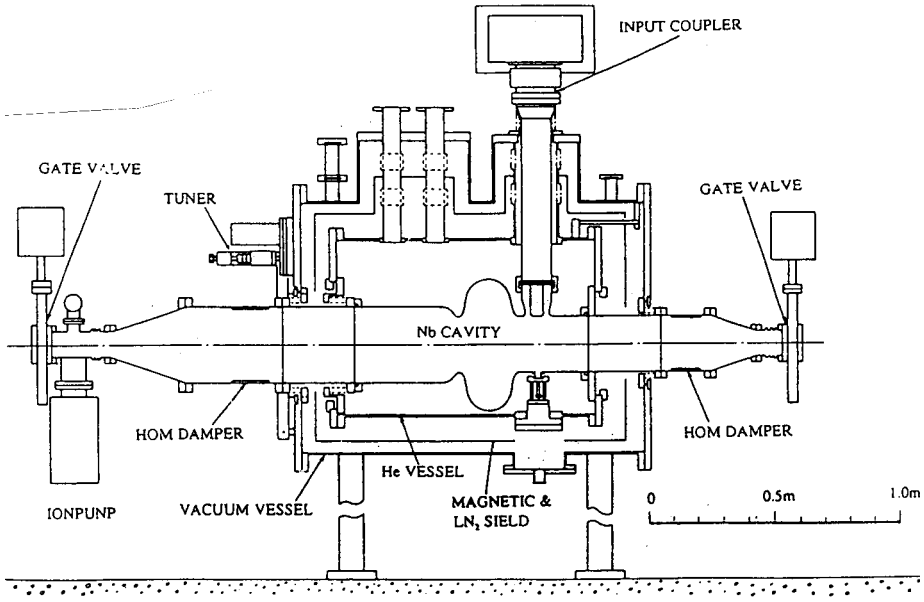

Fig. 5 KEK B-factory accelerating module

3.3 The beam tube RF load

Beam tube HOM couplers have to be terminated into a RF load. If high HOM powers are expected *this load must be at room temperature*. It also must consume little space within the beam tube aperture and should allow cooling to extract the developed heat. The solution which imposes itself is to clad a ring portion of the inner beam tube surface with a uhv-compatible absorbing material. Since, adjacent to a metal surface, only the magnetic field has a component parallel to the absorbing surface layer the material must have *magnetic* RF losses. *Ferrites* are such materials and special uhv compatible ferrites were available from earlier work at CERN [5] to dampen parasitic resonances in the beam pickups of the Antiproton Accumulator. The problem was now to attach such ferrites with a good mechanical and thermal bond to a metal substrate. A technique using soft soldering [6] has been developed at Cornell while KEK [7,8] has succeeded in brazing ferrites. The main obstacle to bonding of ferrites to a metal is their

difference of thermal expansion. It is important to keep the dimensions of ferrite tiles small and to use a ductile metal like copper as substrate. Brazing then can be done in a vacuum oven using a standard Ag-Cu brazing alloy while pressing both partners together with 4 kg/cm^2 force.

3.4 General design implications

The concept of using the beam tubes for HOM damping implies an accelerating-module design where each single-cell cavity is housed in a separate cryostat. As illustrated by the KEK design for a B-factory, the large beam tube sections protrude out of the cryostat to allow ferrite loads at room temperature. The large diameter beam tubes are wide open ports for heat to reach the liquid helium vessel by radiation and conduction. *Obviously the simplicity of the HOM damping scheme has to be paid for by enhanced refrigeration costs.*

3.5 Ferrite beam tube loads for LEP 2

At CERN we[2] prepare ferrite absorbers for mounting them, if required, into the 10-cm diameter beam tube sections between the 4-cavity modules. In LEP 2, once all the copper cavities have been replaced by superconducting ones, the transversal beam impedance will be reduced, so higher bunch charges can be accelerated. In addition, when the particle energy is increased, bunches may become shorter than they are now. As a consequence the HOM power deposition within a module will increase, particularly at high frequencies, where the performance of the HOM couplers is not well known. Figure 6 shows the power spectrum predictions [9] according to the ABCI program. Since this power is deposited into longitudinal modes and since above 2.2 GHz the TM_{01} waveguide mode starts to propagate in a 10-cm diameter tube we can reasonably hope to intercept *the high frequency tail* of the spectrum (about 1 kW for 2 x 4 bunches of 1 mA) at room temperature inbetween the modules.

The ferrite tiles had to be integrated into the pumping boxes between the modules (Fig. 7). The basic idea for their manufacture was first to braze small (3 x 15 x 18 mm^3) ferrite tiles onto flat copper strips which then, by electron beam welding, were joined to form a 10-cm diameter absorber tube. In between the strips 2-mm wide slots allow for pumping. The tube is then integrated into the cylindrical pumping box. Water cooling loops at both ends of the absorber tube remove heat.

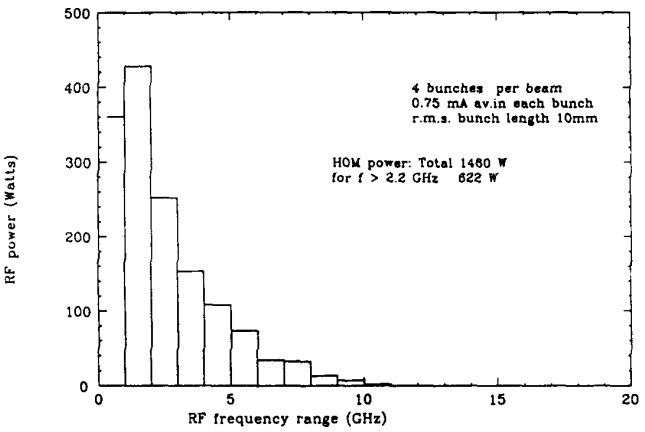

Fig. 6 LEP2 module HOM power from ABCI calculations for σ_s = 10 mm

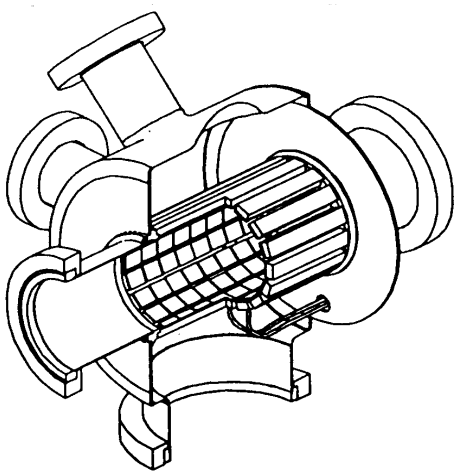

Fig. 7 Pumping box with integrated HOM load

---

[2] F. Caspers, E. Haebel, N. Hilleret, V. Rödel, B. Trincat, R Valbuena

3.6 Concluding remarks on waveguides as HOM couplers and definition of external *Q*

Apart from the technically difficult vacuum RF load, (but which is only needed if the beam tubes themselves are to be used as waveguides), this HOM coupler concept is of great simplicity. We cut an opening into the wall of the cavity and, through this aperture, let RF power radiate into a wave guide which carries the power as a travelling wave to a termination at room temperature. For a mode with angular frequency ω_n , stored energy U_n and radiating the power P_n we may, since $P_n \propto U_n$, characterize the coupling by defining an *external Q* :

$$Q_{\mathrm{ex},n} = \frac{\omega_n U_n}{P_n} \tag{1}$$

Below cut off a guide cannot carry travelling waves. Thus, by a proper choice of the transverse guide dimensions, coupling to the FM is easily suppressed. But guide and cavity dimensions become comparable and integration into a cryostat while keeping heat leaks at an acceptable level is difficult[3]. So *coupling to transmission lines* has become a more widespread technique. We then need a *filter* to suppress FM coupling but we can adapt the line cross-section to the HOM power and minimize heat leaks.

4. COUPLING TO TRANSMISSION LINES AND THE EQUIVALENT-GENERATOR APPROACH

Amongst the different forms of transmission lines the coaxial one is best suited for our purpose. For the moment we will assume that the line is terminated by a matched load, $R=Z_w$, where Z_w is the *wave impedance*, so again energy transport is by a travelling wave.

Let us now examine the interface between cavity and line in more detail. We have two basic choices. As depicted below we can either leave the inner conductor end 'open', forming a *probe*, or 'shorted', forming a *loop*. Seen from the cavity the transmission line terminates this probe or loop by a resistor $R = Z_w$.

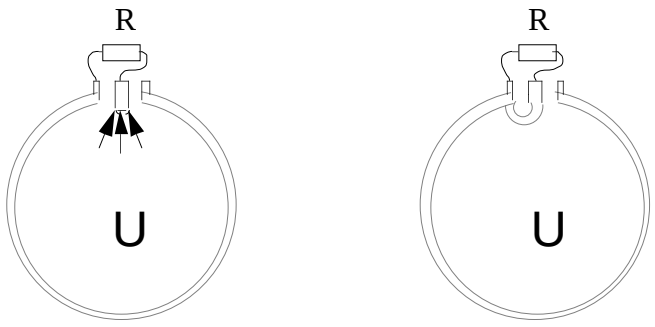

Fig. 8 Two possibilities of coupling, *probe* or *loop*

4.1 Non-resonant coupling

For a given loop or probe the question is now: Which value of R gives the lowest Q_{ex}?

---

[3] At CEBAF HOM couplers in waveguide technique are used but with loads in the liquid He bath, but this is only possible because the HOM power is very small.

To answer the question let a mode at ω be excited by some auxiliary device to oscillate with *constant stored energy U*. We then may regard the probe or the loop as the output port of a RF generator with *emf* V_0 and *internal impedance* Z_i. We can determine V_0 and Z_i by 'measuring' *open circuit voltage* V_0 and *short circuit current* I_0 and have for the loop:

$$I_0 = \frac{\Phi_m}{L_s} = \frac{\mu_0}{L_s} \iint \vec{H} \cdot d\vec{s}$$

$$V_0 = j\omega\Phi_m = j\omega\mu_0 \iint \vec{H} \cdot d\vec{s} \tag{2}$$

L_s is the self-inductance of the loop. H is the mode's magnetic field and we integrate over the loop surface. Evidently $Z_i = j\omega L_s$ and according to *Thevenin's theorem* the coupling port can be described by the *loop inductance* in series with the *induced voltage* as in Fig. 9

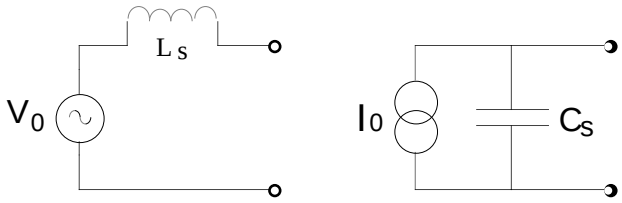

Fig. 9 Equivalent generator circuits for probe and loop coupling

A port equipped with a probe has an equivalent circuit dual to that of the loop. C_s is the fringe field capacitance of the probe tip. I_0 is a short circuit current and corresponds to the displacement current of that part of the cavity *E*-field which ends on the probe surface.

$$I_0 = j\omega\Phi_e = j\omega\varepsilon_0 \iint \vec{E} \cdot d\vec{s} \tag{3}$$

Which power is now extracted from the mode? We find for the *loop* (*Y* is the *admittance* 'seen' by the voltage source V_0):

$$P = \frac{1}{2} V_0^2 \,\mathrm{Re}(Y) = \frac{1}{2} V_0^2 \frac{1}{Z_w} \frac{Z_w^2}{Z_w^2 + (\omega L_s)^2} \tag{4}$$

and for the probe with $Y_w = 1/Z_w$ (*Z* is the *impedance* 'seen' by the current source I_0)

$$P = \frac{1}{2} I_0^2 \mathrm{Re}(Z) = \frac{1}{2} I_0^2 \frac{1}{Y_w} \frac{Y_w^2}{Y_w^2 + (\omega C_s)^2} \tag{5}$$

The presence of L_s (or C_s) diminishes the power flow on the transmission line and hence the damping of the mode.

4.1.1 The limit of obtainable damping

Evidently here we have a dilemma. If, to obtain more damping, we increase the surface of a coupling loop, then also L_s will increase and take away at least part of the potential benefit of the higher induced voltage. And similarly, for a probe a bigger surface will increase C_s.

Let us study this important phenomenon in more detail. We use a geometry of transmission line and loop (see Fig. 10) which hardly would be used in a real construction project but has the advantage that the loop's self-inductance can be expressed by a simple formula. We use a strip line and as loop a *solenoid with only one turn* so (*r* is the radius of the solenoid and *l* its length):

$$L_s \approx \mu_0 \pi \frac{r^2}{l}$$

Figure 11 sketches how such a loop could couple to the TM_{010} mode of a pillbox cavity. The coupler is in the symmetry plane of the cavity and the loop at the equator where the magnetic field *B* is maximal and to first order constant over the loop area. Then:

$$\frac{1}{P} = \frac{2Z_w}{\left(\omega r^2 \pi B\right)^2} \; \frac{Z_w^2 + \left(\omega \mu_0 \pi r^2 / l\right)^2}{Z_w^2}$$

and it follows

$$Q_{\text{ex}} = \frac{\omega U}{P} = 2\frac{\omega U}{B^2}\left\{\frac{Z_w}{\pi^2 \omega^2 r^4} + \frac{\mu_0^2}{l^2 Z_w}\right. \tag{6}$$

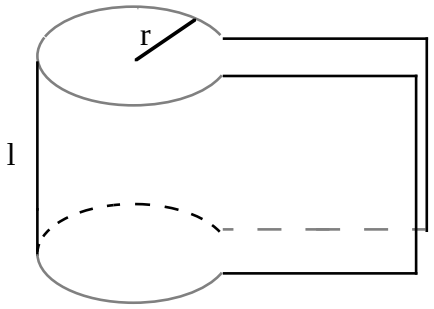

Fig. 10 Stripline with loop of solenoidal geometry

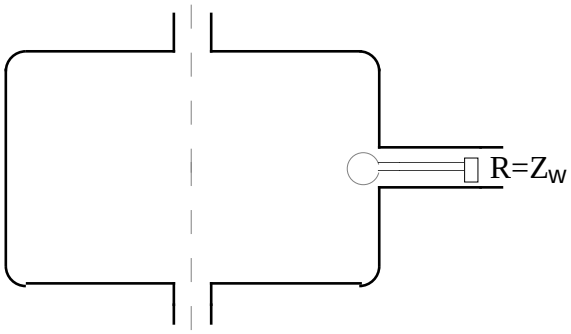

Fig. 11 Pillbox cavity with the coupling loop of Fig. 11 at the equator

The factor $\omega U/B^2$ describes the cavity and loop position, the two additive terms within the curly brackets the coupler itself. The salient point is now that one of the two terms is independent of the loop radius. So it constitutes a lower limit to the obtainable *external Q* (an upper limit of damping). It does not pay to increase the loop radius much beyond the value leading to

$$\frac{Z_w}{\pi^2 \omega^2 r^4} = \frac{\mu_0^2}{l^2 Z_w}$$

But this expression can be rearranged to give

$$\omega L_s = Z_w \tag{7}$$

and in this form is of general validity. Having chosen a wave impedance Z_w for the transmission line and a conductor for the loop, Eq. (7) limits the useful loop size. On the other

hand, as the second term in (6) shows, if the loop area linked to flux remains fixed, increasing the conductor cross-section will lead to improved damping.

An example:

To close this section let us now calculate the *lower external Q limit* for the fundamental mode if we mount this loop coupler on the equator of the 4-cell LEP cavity. For an accelerating voltage of V = 1.7 MV (1 MV/m of accelerating gradient) this cavity has at the equator a magnetic induction of B = 4 mTesla and in the π-mode a (R/Q) of 230 Ω. We now can evaluate $\omega U = V^2/(2R/Q)$ and obtain, for a line impedance of 50 Ω and a loop length of 8 cm, from the second term of Eq. (6):

$$(Q_{ex})_{min} = 3900$$

For the reasonable loop diameter of 4.2 cm which produces ωL_s = 50 Ω, the external Q will be twice the minimal one and increasing the loop diameter by a factor $\sqrt{2}$ to 6 cm we will approach the minimal value to within 25%:

$$Q_{ex} = 5000$$

However, much lower values of Q_{ex} can be obtained from the same loop at the price of some more sophistication.

4.2 Resonant coupling

In the simple non-resonant approach Q_{ex} has a lower limit, since part of the induced voltage is lost as voltage drop across the internal impedance. But this impedance is not resistive as in ordinary generators. For a coupler it is a pure reactance and, in contrast to a resistance, a reactance can most easily be compensated by an opposite one, at least at certain frequencies.

For a loop coupler the simplest measure is to connect a capacitor in series with the loop [10]. If we do so for the 6-cm diameter loop we need a capacitive reactance of 100Ω at 352 MHz. From $1/(\omega C)$ = 100 Ω we obtain C = 4.55 pF. Such a capacity is small enough to be easily realised in practice. The result of compensation is often spectacular. In our example, adding the capacitor would divide the external Q by 5!

$$Q_{ex} = 1000$$

And lower values are within reach as the following discussion will show.

4.2.1 The damping limit for resonant coupling

With the compensation condenser added we have the equivalent circuit of Fig. 12. Evidently now, at the mode frequency, we can increase the extracted power, and hence the damping, if we reduce R (e.g. by connecting a $\lambda/4$ *transformer* between condenser and transmission line) and, in reducing R to zero, it appears as if in the limit Q_{ex} = 0 could be obtained. On the other hand, with R = 0 there are no losses in the system, and Q_{ex} must be infinite! To remove this contradiction we have to realise that, in adding the compensation condenser, we transformed the coupler *itself* into a *resonator* with its own quality factor $Q_{co} = \omega L_s/R$ and tuned to the mode frequency. Figure 13 depicts the situation in representing the mode by a parallel LC-resonator which couples via the mutual inductance $M = k\sqrt{L}\sqrt{L_s}$ to the loop. k is the coupling factor and it follows from the definition of M that the flux of cavity field through the loop is

$$\Phi = M\, I = k\sqrt{L}\sqrt{L_s}\, I$$

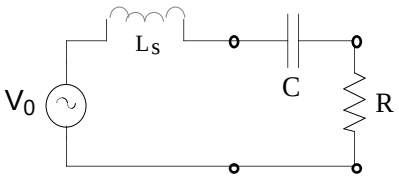

Fig. 12 Capacitive series compensation of loop inductance

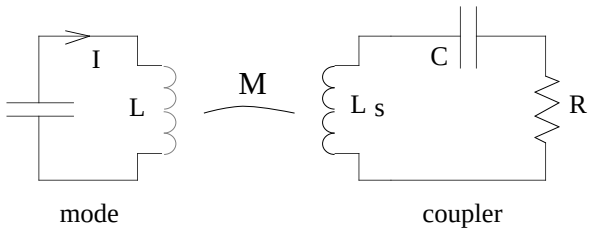

Fig. 13 More realistic representation of coupling

We will now express the previous formulae in a coupled-resonator notation and this will help to see the limit of their range of validity. Using $0.5\,L\,I^2 = U$ we get

$$\Phi^2 = k^2 L_s \cdot LI^2 = 2k^2 L_s U \tag{8}$$

With $P = 0.5V_0^2/R$ we have now

$$P = \frac{1}{2}\frac{(\omega\Phi)^2}{R} = \frac{1}{2}\frac{(\omega\Phi)^2}{\omega L_s} Q_{\mathrm{co}}$$

and substituting from (8) gives

$$P = k^2 \omega U Q_{\mathrm{co}}$$

If now $\omega U/P = Q_{\mathrm{ex}}$ then

$$Q_{\mathrm{ex}} = \left(\frac{1}{k}\right) \cdot \frac{1}{kQ_{\mathrm{co}}} \tag{9}$$

Equation (9) does not give anything new. It still predicts infinite damping for infinite coupler Q. But it is written in the language of coupled-resonator theory which says that for $R = 0$ the presence of the coupler resonator will simply split the cavity mode into two, with frequency difference $\Delta f = k\,f$.

On the other hand, modes of a coupled system are sensitive to perturbations. Damping is one of the possible reasons for perturbations and splitting disappears when $kQ_{\mathrm{co}} < 1$. Substituting this into (9) will give a reasonable estimate of the minimal external cavity Q that can be produced with this resonant coupler technique.

$$(Q_{\mathrm{ex}})_{\min} \approx \frac{1}{k} = \frac{\sqrt{2UL_s}}{\Phi} \tag{10}$$

In our LEP cavity example, with the loop of 6-cm diameter we have $L_s \approx 46$ nH and, for a stored energy of 2.9 Ws, a magnetic flux of $\approx 11.3\ 10^{-6}\ V_s$ through the loop. Using (8) we calculate a coupling factor of $\approx 2\%$ and

$$(Q_{\mathrm{ex}})_{\min} \approx 50$$

The coupler Q must then be 50 too and this requires a resistive termination of 2Ω. In designing couplers for HOM damping one hardly would go to such an extreme because the coupler bandwidth becomes too small and about one coupler per mode would be needed!

4.2.2 Fundamental mode filter requirements

As mentioned earlier coupler constructions based on transmission line techniques have to use a filter to suppress coupling to the fm. This appears to complicate the design but the filter can always be integrated into a reactance compensation scheme. For instance, if in Fig. 12 an inductance $L = L_S$ is connected in parallel to C, then a stop filter for the FM at ω_0 is formed (see Fig. 14). But at higher frequencies the filter reactance becomes capacitive to compensate the loop reactance at $\sqrt{2}\omega_0$. More general for this circuit, if the HOM frequency at which we want compensation is at ω_c then L and C are given by:

$$1/C = \omega_0^2 L = \left(\omega_c^2 - \omega_0^2\right) L_s \qquad (11)$$

Voltage and current in the filter may reach high values. To illustrate this point we do the 'tentative design' of a LEP cavity HOM coupler compensated at 500 MHz and using a loop (as sketched in Fig. 11) with 3-cm diameter and 4-cm length. Then at 352 MHz ωL_s = 50 Ω and, since $500/352 \approx \sqrt{2}$, $L = L_s$. At an accelerating gradient of 6 MV/m the equatorial magnetic cavity field is 24 mT and induces the voltage $\omega\Phi$ = 37.5 kV, which drops across the filter condenser C and drives a current of I = 750 A through L. If C has a gap of 3 mm, (a bigger gap could lead to multipacting), a surface field of 12.5 MV/m results and if the conductor carrying I has a diameter of 3 cm a surface magnetic field of ≈10 mT will be produced, *values comparable to those in the cavity! Construction from superconducting materials using cavity assembly and surface preparation techniques is mandatory.*

Two of the four HOM couplers of the CERN 5-cell 500-MHz prototype sc cavity, built for beam tests in PETRA at DESY, were of this type [11]. An outline of their geometry is given below in Fig. 15. With a coupler $Q \approx 2$ they produced *external Q* values ≈ 40000 and were operated up to accelerating gradients of 4MV/m (limit due to a cavity quench).

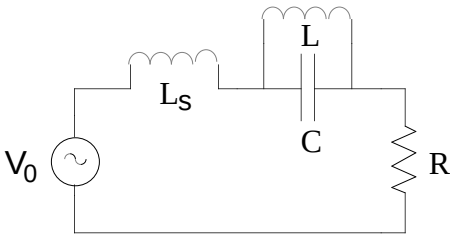

Fig. 14 Resonant HOM coupler with fundamental mode stop filter

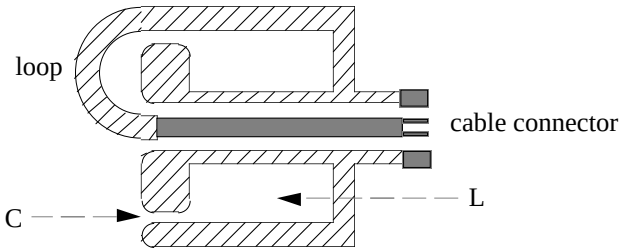

Fig. 15 Outline of resonant HOM loop coupler with FM filter

However, this approach was not further pursued for two reasons. Making an opening at the cavity equator causes local field enhancement just where the FM B-field has its maximum, and putting the coupler at the maximum in turn causes very high field values in the coupler's filter. Looking for a coupler position with smaller FM field and above all a more favourable ratio of HOM to FM fields, a *position on the beam tubes* of the cavity was identified as optimal. The TM_{01} mode being in cut off, damping in the beam tube then acts as a prefilter for the FM .

4.2.3 Couplers on the beam tube with several resonances

Another feature of the last generation of HOM coupler designs is that they are tailored to be resonant at *several* frequencies. Figure 16 illustrates for the LEP cavity the distribution of

HOM with significant *R/Q* values. As we see, high *R/Q* HOM come in three clusters around 480 MHz, 650 MHz and 1.1 GHz, so at these frequencies should be resonances of the HOM coupler. A heuristic approach leading to a coupler with the required three resonances is the following. First realize that 650 and 1100 MHz are nearly harmonic and that a transmission line resonator of length λ/2 at 650 MHz with shorts at both ends would have a second resonance at 1300 MHz.

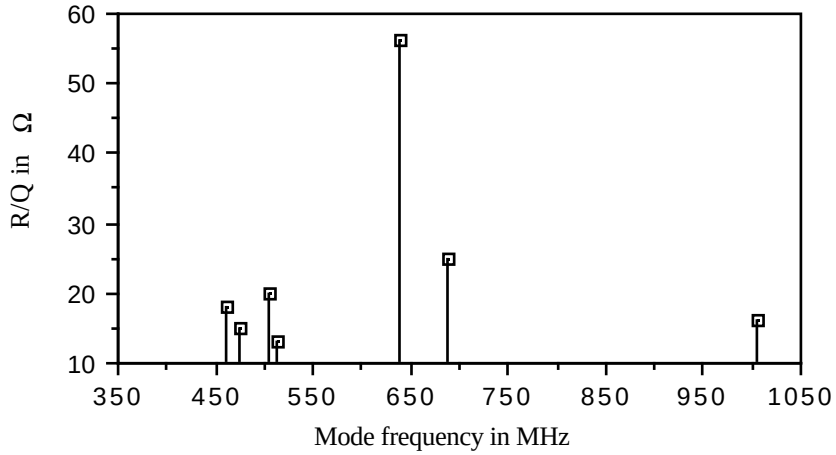

Fig. 16 The high *R/Q* HOM of the LEP cavity

Replacing the shorts by small inductances L_1 & L_2, (and L_1 would be the coupling loop), we can move these resonances nearer to each other. A third lower frequency resonance finally is obtained by connecting the termination *R* (see Fig. 17) via a capacitor *C* to L_2. L_2, *C* and *R* then form a second resonator, which shares with the line resonator the common element L_2. In other words: the two resonators are coupled, allowing to split the original 650 MHz resonance into two.

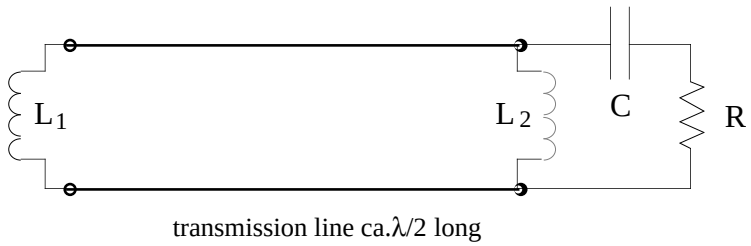

Fig. 17 Circuit of a transmission line coupler with three resonances

The HOM couplers [12] used at DESY in HERA and more recently in the TESLA [13,14] project, as well as at CERN on the LEP Nb-Cu cavities all use this approach. As shown in Fig. 18 the HERA coupler has a small antenna added to the loop so that coupling to electric cavity fields is enhanced. The FM filter is in the back of the coupler, parallel to L_2, forcing a voltage zero across *C*. In CERN (see Fig. 19) the filter has been moved to the front in returning L_1 via a capacitor to ground. In this way coupling to FM *E*-fields is eliminated. Also, to avoid magnetic coupling, the loop is perpendicular to the cavity axis. HOM coupling is electric for the longitudinal modes and predominantly magnetic (to their B_z in the beam tube) for the dipole modes. This modification made it possible to have a *demounting flange*, which has to carry only the HOM power. In fact, for a successful fabrication of sc cavities by sputter-coating [15], demountability of couplers is a precondition.

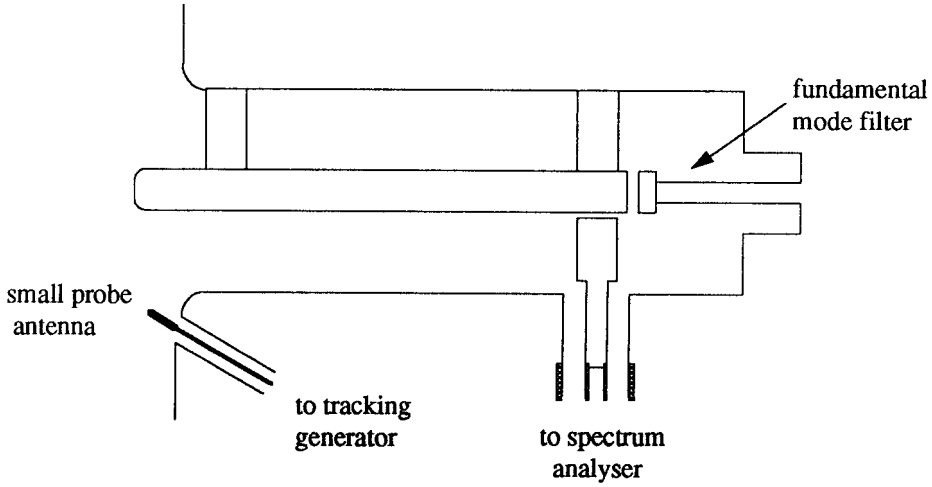

Fig. 18 Scheme of the HERA HOM coupler

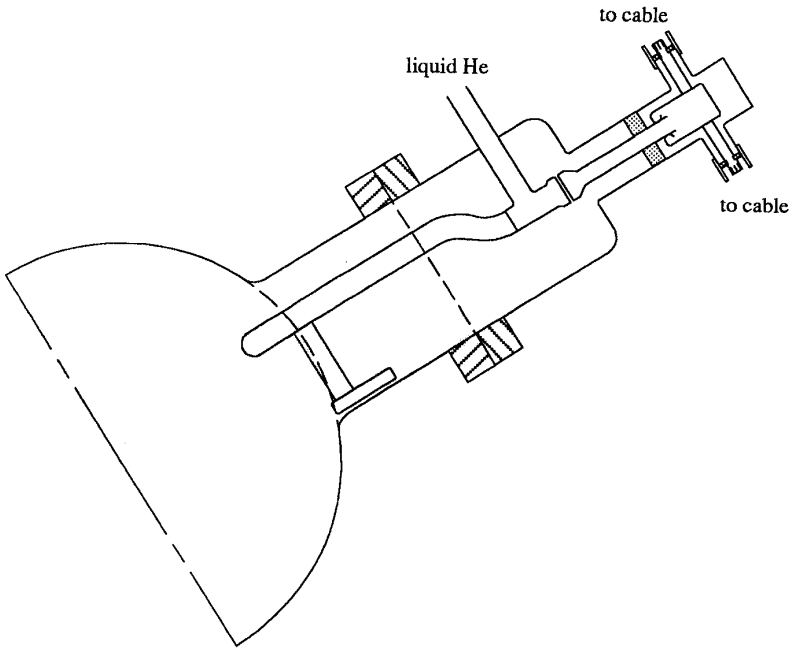

Fig. 19 Demountable coupler for sputter-coated LEP cavities

At SACLAY and CERN it has also been found that letting a loop protrude into the beam tube is another way to get sufficient coupling to the *E-fields* of the longitudinal (TM_{0nm}) modes. This is an interesting variant since it is simpler to fabricate and has been chosen for the LEP cavities. A schematic drawing together with a table of external Q_s is given in Appendix A.

4.3 Design aids

The equivalent generator approach combined with a circuit model of the coupler lends itself readily to making meaningful estimations of mode damping. One ingredient is a calculation (by a network analysis code) of the real part of the coupler's input impedance for probes (or admittance for loops) *including* into the network the coupler's C_s (or L_s respectively).

The second ingredient is an estimation of the probe's short-circuit current I_0 (or the loop's open-circuit voltage V_0) with the help of a cavity code which gives the stored energy U and the fields E and H at the coupler's location. We assume that these fields are not too much perturbed by the presence of the coupler, and estimating the integrals of (2) and (3) we have all the needed information to calculate Q_{ex}.

During the conceptual design phase of a HOM coupler it is most useful to plot the calculated real part of the input impedance (or admittance) against frequency to identify the position of maxima (resonances) and their relative height. After building hardware models such 'sensitivity' curves can be verified in measuring the transfer function between a small loop or probe (which replace the cavity field) and the coupler's load as illustrated in Fig. 18.

More recently a code (HFSS) has become available which, with the exclusion of the interaction region between coupler and cavity fields, allows one to calculate the s-parameters of a complete hardware model. Using it greatly facilitates the translation from the circuit model to the final RF structure.

5. THE HIGHER ORDER MODE POWER

Obviously a good knowledge of the HOM power is needed if one has to decide on the size of the couplers and of cables, connectors and vacuum feedthroughs which serve to connect the couplers to room temperature loads.

5.1 Beam with sinusoidally varying linear charge density

To calculate the RF power (Ref. [16] contains a more general treatment of the subject) from a particular mode with frequency ω_m first imagine a beam with sinusoidally varying linear charge density which passes an AC current I with frequency ω through a reference plane of the cavity exciting oscillating fields of the same frequency. If ω is in the vicinity of ω_m this mode's field will predominate with an amplitude depending on ω as typical for a resonance, i.e. reaching at $\omega = \omega_m$ a maximum proportional to I. We may measure the accelerating effect of the field by test charges (which have the same speed $v \approx c$ aas the paticles of the beam) and call the *factor of proportionality* between the found *accelerating voltage* V and I (at $\omega = \omega_m$) the *effective shunt impedance R.*

$$V = R\, I \tag{12}$$

R in turn is proportional to the loaded Q of the mode and we call the factor of proportionality *(R/Q).*

$$R = \left(\frac{R}{Q}\right) Q \tag{13}$$

The method used to define V implies for the power P_m lost by the beam at resonance to the mode's field:

$$P_m = \frac{1}{2} I\, V$$

using (12) it follows that

$$P_m = \frac{1}{2} \frac{V^2}{R}$$

But conservation of energy demands that P_m is equal to the power dissipated in the cavity walls and in the HOM coupler load

$$P_{\text{diss}} = P_m = \frac{1}{2}\frac{V^2}{R} \tag{14}$$

Further by definition

$$Q = \frac{\omega U}{P_{\text{diss}}} \tag{15}$$

where U is the stored energy of the mode. Combining (11), (12) and (13) gives:

$$\left(\frac{R}{Q}\right) = \frac{1}{2}\frac{V^2}{\omega U} \tag{16}$$

Using a cavity code (SUPERFISH, URMEL, MAFIA…) *(R/Q)* can be calculated from Eq. 16 for all non-propagating modes and P_m could be determined for given I and Q. But it is more important to realise that all these equations map on the circuit equations of a parallel LC-resonator (see Fig. 20) to which the beam current is connected in the form of a current source and which has $1/(\omega_m C) = (R/Q)$.

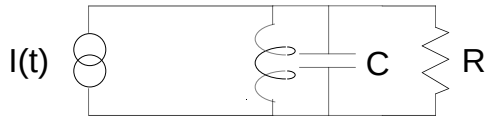

Fig. 20 Circuit model of beam-mode interaction

Trusting the equivalence between circuit model and mode we can now determine the response of the mode *to other beam current forms.*

5.2 Response to a single bunch

For a point charge q passing the reference plane at $t = 0$ the beam current has the form of a single δ-current pulse.

$$I(t) = q\,\delta(t)$$

Such a pulse charges the condenser discontinuously to the voltage q/C which, if the condenser had no charge before, is the initial amplitude of a subsequent *free oscillation*:

$$V(t) = q\,h(t) \quad \textit{with} \qquad h(t) = \frac{u(t)}{C}e^{\gamma t}$$

$u(t)$ is the unit step function.

With the filling time T_f:

$$\gamma = -\frac{1}{T_f} + j\omega_m = -\frac{\omega_m}{2Q} + j\omega_m$$

Further, for a ***linear*** system such as the circuit here and *any* beam current $I(t)$

$$V(t) = \int_{-\infty}^{\infty} I(\tau)\, h(t-\tau)\, d\tau$$

and for our $h(t)$: $$V(t) = \frac{e^{\gamma t}}{C} \int_{-\infty}^{\infty} I(\tau)\, u(t-\tau)\, e^{-\gamma\tau} d\tau \qquad (17)$$

We now examine a *single* beam-current pulse $I(\tau)$ and $V(t)$ at times t when the current has returned to zero. During the pulse then $u(t - \tau) = 1$. Also, in accelerators the beam current pulses are very short compared to $2Q/\omega_m$. So it makes no difference if we neglect the attenuation and replace the integral in (17) by

$$\int_{-\infty}^{\infty} I(\tau) e^{-j\omega_m \tau} d\tau$$

This is the Fourier transform of the current pulse $I(t)$ at ω_m. A single gaussian bunch of charge q with

$$I(t) = \frac{q}{\sqrt{2\pi}} \frac{1}{\sigma} e^{-\frac{1}{2}\frac{t^2}{\sigma^2}}$$

has the Fourier transform

$$I(\omega) = q e^{-\frac{(\omega\sigma)^2}{2}}$$

and ***after*** *the passage* of a single gaussian bunch

$$V(t) = V_b\, e^{\gamma t} \qquad (18)$$

with $$V_b = \omega_m \left(\frac{R}{Q}\right) e^{-\frac{(\omega_m \sigma)^2}{2}} \quad q \qquad (19)$$

5.3 The HOM voltage due to a bunched beam

We may now go a step further and try to determine the response to a *beam* made up of bunched charges q which, passing through the reference plane, constitute a *pulsed current with period* T_b. In a steady state the excited oscillations must have the same period T_b . On the other hand, in between bunch passages the mode oscillations must be *free* oscillations i.e. representable by a *phasor* V turning with angular speed ω_m.

Formally, we may turn this phasor back or forward to the moment of the last or next bunch passage and in this way construct phasors V_+ and V_- . Further, to have the required overall periodicity with T_b, at the moment of a bunch passage, the accelerating voltage induced by the bunch must update V_- to become V_+. Central to the derivation is now that, due to the *linearity* of the circuit, this updating voltage must be V_b. Writing complex quantities with a tilde:

$$\tilde{V}_+ = \tilde{V}_- + V_b$$

but also $\tilde{V}_- = \tilde{V}_+ e^{\gamma T_b}$

$$\tilde{V}_+ = V_b \frac{1}{1 - e^{\gamma T_b}}$$

and for the time interval of free oscillations:

$$\tilde{V}(t) = V_b \frac{e^{\gamma t}}{1 - e^{\gamma T_b}} \qquad for \qquad 0 < t < T_b \tag{20}$$

5.4 The HOM power from a bunched beam

$\tilde{V}(t)$ drops across the shunt impedance R, causing in average the dissipation

$$P_{\text{mode}} = \frac{1}{2}\frac{1}{T_b}\int_0^{T_b} \frac{\left|\tilde{V}(t)\right|^2}{R}\, dt$$

P_{mode} is furnished by the bunched beam. Substituting (20)

$$P_{\text{mode}} = \frac{V_b^2}{2RT_b\left|1 - \exp(\gamma T_b)\right|^2} \int_0^{T_b} \mathrm{e}^{-\frac{2t}{T_f}}\, dt$$

using $\tau = \dfrac{T_b}{T_f} = \dfrac{\omega_m T_b}{2Q}$ *and* $\delta = \omega_m T_b$ (*modulo* 2π)

we have $\left|1 - \exp(\gamma T_b)\right|^2 = 1 - 2\cos\delta\ \exp(-\tau) + \exp(-2\tau)$

And evaluating the integral we obtain with $R = Q(R/Q)$ the result:

$$P_{\text{mode}} = \frac{\frac{1}{2}V_b^2}{\left(R/Q\right)}\ \frac{1}{\omega_m T_b}\ \mathrm{F}(\tau,\delta) \tag{21}$$

where $$\mathrm{F}(\tau,\delta) = \frac{\left(1 - \exp(-\tau)\right)\left(1 + \exp(-\tau)\right)}{1 - 2\cos\delta\ \exp(-\tau) + \exp(-2\tau)} \tag{22}$$

For gaussian bunches of charge q and substituting from (19)

$$P_{\text{mode}} = \frac{1}{T_b} k_m\, q^2\ \mathrm{F}(\tau,\delta) \tag{23}$$

k_m is called the loss parameter [16] of the mode at ω_m.

$$k_m = \frac{1}{2}\omega_m \left(\frac{R}{Q}\right) \mathrm{e}^{-(\omega_m \sigma)^2} \tag{24}$$

The pulsed current of a bunched beam corresponds to a spectrum of discrete lines at distance $1/T_b$ which has the Fourier transform of a single pulse as envelope curve. $\delta = 0$ (modulo 2π) means that ω_m coincides with one of the spectral frequencies. At $\delta = \pi$ the mode is just in between two spectral lines. Figure 21 shows a plot of $F(\tau,\delta)$ for these two cases. Note that $F(\tau,\pi) = 1/F(\tau,0)$. F is plotted against $2/\tau = 4Q/(\omega_m T_b)$.

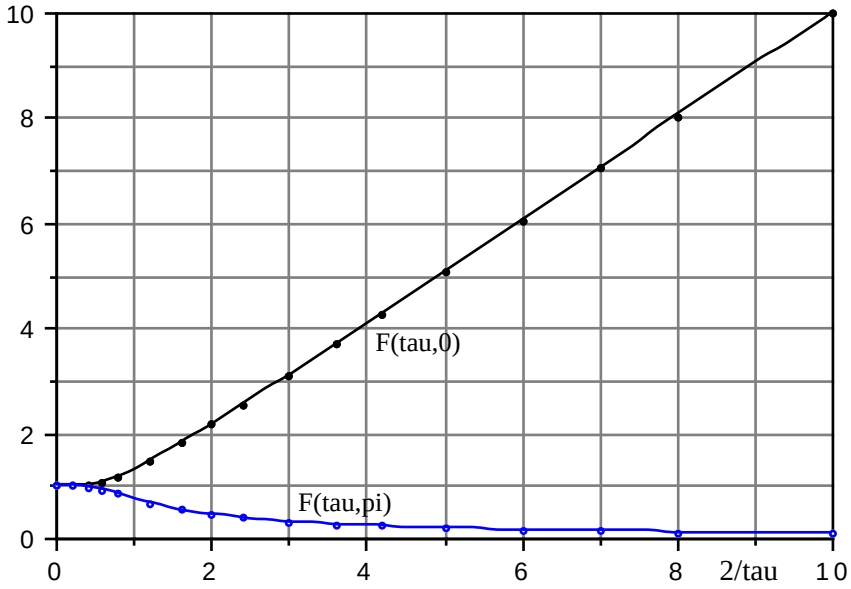

Fig. 21 F(τ,0) and F(τ,π) plotted against $2/\tau = 4Q/(\omega_m T_b)$

5.4.1 The strong damping limit

Whatever the δ, for increasing damping (increasing τ) F approaches one, and P_{mode} becomes

$$P_{\text{mode}} \approx \frac{1}{T_b} k_m q^2 \tag{25}$$

In the limit each bunch of the beam sees an "empty" cavity and we conclude that the bunches now loose an energy $k_m q^2$ to each mode. For strong damping of all HOM the expression for the total HOM power thus must have the simple form

$$P_{\text{HOM}} \approx \frac{1}{T_b} k q^2 \tag{26}$$

with

$$k = \sum k_m \tag{27}$$

If the beam is kept on the cavity axis where transversal modes have no accelerating field, only longitudinal modes contribute to k. Codes like TBCI and ABCI allow one to calculate the k_m and their sum, even including the frequency range where modes propagate.

5.4.2 The weak damping limit

If $\tau = 0.5\omega_m T_b/Q$ is small enough to approximate $\exp(-\tau)$ by $1-\tau$ then we can simplify setting:

$$F(\tau,0) \approx \frac{2}{\tau} = \frac{4Q}{\omega_m T_b}$$

Formula (21) now takes the form

$$P_{\text{mode}} \approx \frac{1}{2}\left(\frac{2q}{T_b} e^{-\frac{1}{2}(\omega_m \sigma)^2}\right)^2 \left(\frac{R}{Q}\right) Q$$

The expression in brackets is the intensity of the beam current's spectral line at ω_m. Calling it the beam's RF current at ω_m we have:

$$P_{\text{mode}} \approx \frac{1}{2} I_{\text{rf}}^2 \left(\frac{R}{Q}\right) Q = \frac{1}{2} I_{\text{rf}}^2 R \qquad (28)$$

We arrived at a formula rigourously valid for a *single* harmonic current source and conclude that used for a bunched beam this approximation is better the smaller the mode's loaded bandwidth compared to $1/T_b$.

5.5 Choices of damping

As we have seen, for a bunched beam we can never reduce the HOM power to zero. The lower limit of power given by (26) is the higher the smaller the number of bunches circulating in a machine for a given average DC beam current $I_0 = q/T_b$. In fact, by substitution of I_0 into (26):

$$P_{\text{HOM}} = k I_0^2 T_b \qquad (29)$$

Small numbers of bunches also produce a dense spectrum of beam lines, so the scatter of HOM frequencies due to dimensional tolerances of cavity production may become comparable to $1/T_b$. It is then impossible to avoid resonances between modes and beam lines and filling times T_f should be made equal or smaller than T_b at least for longitudinal modes with significant *(R/Q)* values.

On the other hand, if high numbers of equally spaced bunches circulate in a machine it may be possible to detune high *(R/Q)* modes from beam lines and weak damping gives an advantage, provided beam stability requirements allow high external *Q* values. In all these cases the resulting *loaded Q* will be many orders of magnitude smaller than the Q_0 of modes in a sc cavity. So HOM dissipation in the cavity walls will be negligible compared to the dissipation due to the generator driven fundamental mode.

6. THE FUNDAMENTAL MODE POWER COUPLER

6.1 Matching

Power couplers must have specified properties only near to a single frequency. In this respect they differ considerably from HOM couplers, which in general have to cover broader

frequency ranges. Also, at least for the applications developed so far, they must couple only loosely to the fm. If again we measure coupling by an external Q, values smaller than 1E+5 will hardly be needed and reactance compensation techniques to enhance coupling are not required, rather *'matching'* is required.

The concept of *matching* comprises measures which, by an appropriate choice of impedances, optimize the generation and the transport of power. A simple high power RF system has three building blocks: the power amplifier, a line (transmission line or wave guide) and the load. We then want to minimize power losses on the line. This implies that power is transported by a pure traveling wave and so the line must see a load equal to its wave impedance. In most cases, to realise this condition, we need to connect special impedance transforming *matching devices* between the line and the load proper and to produce a *'load match'* is one of the functions of the power coupler.

Another matching task is at the output port of the power amplifier which, for best efficiency, must work on a tightly specified resistive termination. If lines of standard wave impedance Z_0 are used, the needed transformers form part of the amplifier circuit. The system is now in a state where it works with highest efficiency, but more matching can be done to improve its behaviour in the presence of load matching *errors*. The problem is that klystron and tetrode power amplifiers have an internal or 'source' resistance, which may be an order of magnitude higher than their optimal load resistance. Hence, looking back to the amplifier, the line is not matched. This has the consequence that reflections at the load are back reflected from the amplifier adding to the forward power which thus depends on the load. Matching at the amplifier side of the line is called *'source matching'*. At microwave frequencies a convenient way of source matching is to connect a *circulator* between amplifier and line. For a fixed drive power to the amplifier the forward power is then independent of load matching errors.

6.2 Matching the external Q

The load to which a power coupler shall match is a special one: The FM of a sc cavity, which exchanges energy with the bunches of a particle beam. If we represent the mode by a parallel LC resonator (with $\omega_c L = 1/(\omega_c C) = (R/Q)$) then the beam is a current source connected to its terminals. In the discussion here, which focuses on matching, it is sufficient to regard the coupler as an impedance transformer for the wave impedance Z_0 of the line, so that looking from the resonator to the line we see a transformed wave impedance Z (see Fig. 22).

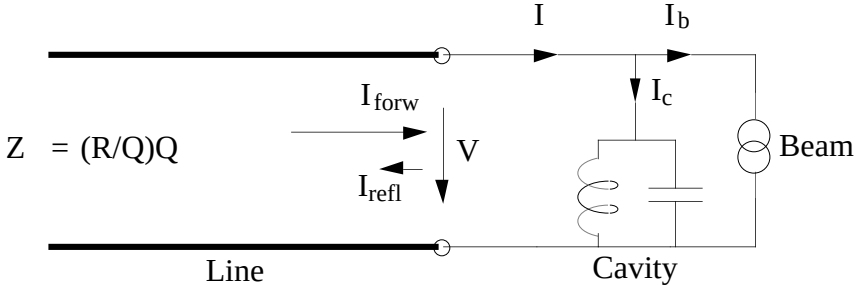

Fig. 22 Line with attached equivalent circuit of loss-free cavity and beam

If this line is source matched then, *seen from the resonator*, its input impedance is also Z, producing as *external Q*

$$Q = \omega_c C\, Z = (R/Q)^{-1}\, Z \tag{30}$$

We will now assume that the resulting bandwidth $\Delta\omega_c = \omega_c/Q$ is small compared to the bunch frequency. With the resonator tuned near to one particular line of the beam current's spectrum the voltage due to all other lines may then be neglected i.e. the current source in Fig. 22 can be thought of as emitting a *sinusoidal* RF current of frequency ω_g, identical to that of the RF power generator.

In the following derivations we will write complex variables (phasors) with a tilde, their modules (amplitudes) and other real quantities without.

The circuit equations are here:

$$\tilde{V}_{\text{forw}} + \tilde{V}_{\text{refl}} = \tilde{V}$$

and

$$\tilde{I}_{\text{forw}} - \tilde{I}_{\text{refl}} = \tilde{I} = \tilde{I}_c + \tilde{I}_b \tag{31}$$

$$2\tilde{I}_{\text{forw}} = (\tilde{I}_{\text{forw}} + \tilde{I}_{\text{refl}}) + \tilde{I}_c + \tilde{I}_b$$

but $I_{\text{forw}} + I_{\text{refl}} = (V_{\text{forw}} + V_{\text{refl}}) / Z = V / Z$ and $\tilde{I}_c = \tilde{V} / \tilde{Z}_c$

$$2\tilde{I}_{\text{forw}} = \tilde{V}\left(\frac{1}{Z} + \frac{1}{\tilde{Z}_c}\right) + \tilde{I}_b \tag{32}$$

where

$$\frac{1}{\tilde{Z}_c} = j\left(\frac{\omega_g}{\omega_c} - \frac{\omega_c}{\omega_g}\right)\left(\frac{R}{Q}\right)^{-1} \tag{33}$$

Equation (32) is a relation between phasors in a complex current plane. If now we wish to represent (32) by a *phasor diagram*, we are free to define the time zero and thus to decide which of the phasors shall be collinear with the real axis.

- Accelerator physicists often declare the RF beam current as real. In fact it appears natural to regard bunch charges as real quantities and hence also the resulting beam current.

- Circuit analysis usually takes the generator signal, here the forward current, as reference and regards it as real.

- For people who develop sc cavities, the accelerating voltage is a main concern. Regarding it as the reference has advantages. The cavity current I_c (since we neglect cavity losses) is now an imaginary quantity for any tuning and the angle of the RF beam current phasor gives directly the synchronous phase Φ *if we use the convention to count it from the crest of the cavity voltage.* But the forward current now is in general complex and the expressions which relate forward and beam power are under general conditions, rather complicated.

In the following we need to find the optimal conditions for power transfer to the beam. We regard an *'accelerating station'* i.e. a *group of cavities* which, from a power divider, all receive the *same forward power*. Also, the distance of cavities on the beam axis has been chosen to make for all of them the beam current phasor equal in amplitude and phase which, *referenced to the forward current*, is called *'station phase'* φ. Under these conditions it is most convenient to regard the forward current as a real quantity, as in the *phasor diagram* of Fig. 23.

Since Z is real but $\tilde{Z}_c$ imaginary, the phasors $\tilde{V} / Z$ and $\tilde{V} / \tilde{Z}_c$ are at a right angle and meet on a circle which has $2I_{\text{forw}} - \tilde{I}_b$ as diameter. Figure 23 represents a non matched situation: both cavity detuning and coupling are incorrect. To match we first retouch the detuning so that $\tilde{V}$ becomes collinear with I_{forw} (the line 'sees' a real impedance). The result is shown in Fig. 24:

$I_c = V/Z_c$ now compensates the imaginary component I_{bi} of the beam current and if we substitute Z_c from (33) we get the detuning condition

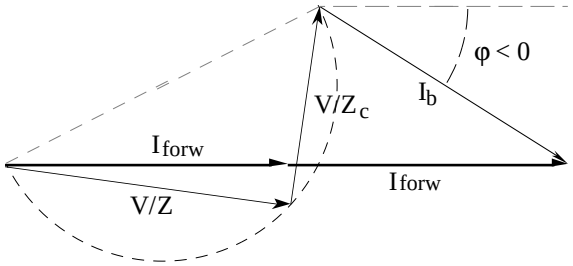

Fig. 23 Equation (32) in a phasor diagram representation

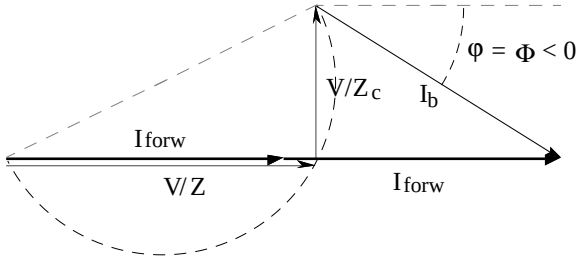

Fig. 24 Phasor sum for a correct cavity detuning

$$I_c = \frac{V}{Z_c} = V\left(\frac{\omega_g}{\omega_c} - \frac{\omega_c}{\omega_g}\right)\left(\frac{R}{Q}\right)^{-1} = -I_{bi} = -I_b \sin\Phi \tag{34a}$$

or

$$\frac{(\omega_g - \omega_c)}{0.5(\omega_c/Q)} \approx -Q\left(\frac{R}{Q}\right)\frac{I_b}{V}\sin\Phi \tag{34b}$$

ω_c/Q is equal to the loaded 3dB bandwidth $\Delta\omega_c$ if the line which feeds power to the cavity is source matched. When (34) is satisfied, station phase φ and synchronous phase Φ *(measured from the crest of the cavity voltage)* become equal.

If the detuning condition is met, Eq. (31) reads:

$$I_{\text{forw}} - \tilde{I}_{\text{refl}} = I_{br} = I_b \cos\Phi$$

and to obtain zero reflection we have in addition to satisfy $I_{\text{forw}} = I_{br}$. But for zero reflection we have also $V = V_{\text{forw}}$. Thus (since $Z_m = (R/Q)Q$):

$$V = V_{\text{forw}} = I_{\text{forw}} Z_m = I_{\text{br}}\left(R/Q\right)Q_m$$

Solving for Q_m and using $2P_b = V I_{br}$ we obtain the condition in a more practical form:

$$Q_m = \frac{1}{2}\frac{V^2}{P_b}\left(R/Q\right)^{-1} \tag{35}$$

P_b is the power transferred to the beam. Note that, for a given cavity voltage amplitude, Q_m depends only on P_b and not on the particular combination of beam current and synchronous phase angle which produces P_b . The phasor diagram for the matched case is shown in Fig. 25 below:

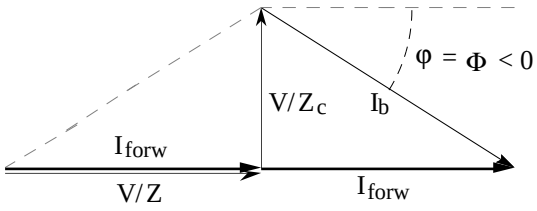

Fig. 25 Phasor diagram at the match point

Example:

The cavities in LEP2 work at 10.2 MV (6 MV/m) and transfer 120 kW to the beam. With (R/Q) = 230 Ω we calculate from (35) Q_m = 1.9E6. The corresponding 3 dB *bandwidth* is 187 Hz. The RF beam current is 28 mA and the synchronous phase -32.8°. Measured in units of half a bandwidth the required cavity detuning is then 0.64 .

6.2 Matching error analysis

In the following we will use a more formal way of analysis to discuss also the consequences of *matching errors*. Introducing normalized values of detuning, beam current and cavity voltage:

$$d = Q\left(\frac{\omega_g}{\omega_c} - \frac{\omega_c}{\omega_g}\right) \approx \frac{\left(\omega_g - \omega_c\right)}{0.5\Delta\omega_c} \qquad \tilde{i}_b = \frac{I_b}{I_{\text{forw}}} = i_{br} + \mathrm{j}\, i_{bi} \qquad \text{and} \qquad \tilde{v} = \frac{\tilde{V}}{V_{\text{forw}}}$$

and solving (32) and (33) for $\tilde{V}$ we get:

$$\tilde{v} = \frac{2 - \tilde{i}_b}{1 + \mathrm{j}d} = \frac{(2 - i_{br}) - \mathrm{j}\, i_{bi}}{1 + \mathrm{j}d} \tag{36}$$

and calculate from $\tilde{V}$ the reflection coefficient $\tilde{\rho}$.

$$\tilde{\rho} = \frac{\tilde{V}_{\text{refl}}}{V_{\text{forw}}} = \frac{\tilde{V} - V_{\text{forw}}}{V_{\text{forw}}} = \tilde{v} - 1 = \frac{(1 - i_{br}) - \mathrm{j}(d + i_{bi})}{1 + \mathrm{j}d} \tag{37}$$

Let the cavity detuning at which $\tilde{V}$ and $\tilde{\rho}$ become real be d_0. At d_0 the expressions in the denominator and nominator of (36) must have equal phases:

$$\frac{d_0}{1} = -\frac{i_{bi}}{2 - i_{br}}$$

and if we substitute this result back:

$$v = \left(2 - i_{br}\right) \tag{38}$$

and

$$\rho = 1 - i_{br} \tag{39}$$

Evidently complete matching is obtained if, in addition to $d = d_0$, also $i_{br} = 1$.

Finally, to evaluate also for the general non-matched case the power P_b transfered to the beam we determine $1-|\rho|^2$. From (37):

$$|\rho|^2 = \frac{\left(1 - i_{br}\right)^2 + \left(d + i_{bi}\right)^2}{1 + d^2} \tag{40}$$

$$\boxed{\frac{P_b}{P} = 1 - |\rho|^2 = \frac{i_{br}\left(2 - i_{br}\right) - i_{bi}\left(2d + i_{bi}\right)}{1 + d^2}} \tag{41}$$

P is the forward power needed to transfer P_b to the beam.

6.2.1 Coupling errors

Let us now compare two cavities of the accelerating station. One, the reference cavity, shall be matched i.e. have (P_m is the forward power and I_{brm} the real component of the RF beam current phasor):

$$I_{\mathrm{brm}} = \left(I_{\mathrm{forw}}\right)_m = \sqrt{2P_m} \,/\, \sqrt{Z_m} \quad \Rightarrow \quad \sqrt{2P_m} = I_{\mathrm{brm}} \sqrt{Z_m}$$

$$\text{and} \quad V_m = \left(V_{\mathrm{forw}}\right)_m = \sqrt{2P_m}\sqrt{Z_m} \quad \Rightarrow \quad \sqrt{2P_m} = \mathrm{V_m} \,/\, \sqrt{Z_m}$$

The second cavity shall be correctly detuned ($d = d_0$) and sees the same RF beam current. But with $Z \neq Z_m$ it will receive from its line a different value of forward current and of forward voltage:

$$I_{\mathrm{forw}} = \frac{\sqrt{2P_m}}{\sqrt{Z}} = I_{\mathrm{brm}} \sqrt{\frac{\mathrm{Z_m}}{\mathrm{Z}}} \quad \Rightarrow \quad \mathrm{i_{br}} = \frac{I_{\mathrm{brm}}}{I_{\mathrm{forw}}} = \sqrt{\frac{Z}{Z_m}} = \sqrt{\frac{Q}{Q_m}}$$

$$\text{and} \qquad V_{\mathrm{forw}} = \sqrt{2P_m}\sqrt{Z} = V_m \sqrt{\frac{Z}{Z_m}} = V_m \sqrt{\frac{Q}{Q_m}}$$

Substituting into (39) and (38) we find for the second non-matched cavity:

$$\rho = 1 - \sqrt{\frac{Q}{Q_m}} \tag{42}$$

and for the ratio of cavity voltages:

$$\boxed{\frac{V}{V_m} = \sqrt{\frac{Q}{Q_m}}\left(2 - \sqrt{\frac{Q}{Q_m}}\right)} \tag{43}$$

From $P_b = (1 - |\rho|^2)\, P_m$ we verify that (43) also describes the ratio of powers transferred to the beam. P_b does not vary strongly with Q. For $Q/Q_m = \sqrt{2}$ we find $P_b/P_m = 0.964$.

A more serious consequence of a coupling error is increased voltage in the coupler's transmission line. V_{refl} adds to V_{forw} to form a standing wave pattern with voltage maxima of $V_{\mathrm{max}} = (1+|\rho|)\, V_{\mathrm{forw}}$. Here we must differentiate between two cases: overcoupling, $Q < Q_m$, and undercoupling, $Q > Q_m$:

$$1 + |\rho| = \begin{cases} 2 - \sqrt{Q/Q_m} & \text{when} \quad Q \le Q_m \\ \sqrt{Q/Q_m} & \text{when} \quad Q > Q_m \end{cases} \tag{44}$$

Present day couplers work at field levels far below those found in cavities. So, why is increased voltage a problem? The answer is that, in contrast to sc cavities, power couplers may be plagued by multipacting discharges within their operating power range and that, in the presence of mismatch, the forward power at which a given multipacting resonance is met, becomes reduced by $(1 + |\rho|)^2$.

Example:
If, with the important mismatch of $Q/Q_m = \sqrt{2}$, one sends 120 kW to the cavity one loses only the moderate reflected power of 4.3 kW. But multipacting levels up to an equivalent power of 170 kW are now within the operating range of the coupler!

6.2.2 Beam current changes

We now change the real component of the RF beam current from I_{brm} to I_{br} and simultaneously, by a servo loop, the forward power from P_m to P *so that the voltage of the reference cavity stays constant.* Equation (38) then gives the condition for the changed forward current:

$$V = V_{\mathrm{forw}}\left(2 - i_{\mathrm{br}}\right) = I_{\mathrm{forw}} Z_m \left(2 - \frac{I_{\mathrm{br}}}{I_{\mathrm{forw}}}\right) \equiv V_m = I_{\mathrm{brm}} Z_m$$

or
$$2 I_{\mathrm{forw}} = I_{\mathrm{br}} + I_{\mathrm{brm}} \tag{45}$$

and remembering that $I_{\mathrm{brm}} = (I_{\mathrm{forw}})_{\mathrm{m}}$ we have

$$I_{\mathrm{forw}} = \frac{1}{2} I_{\mathrm{brm}} \left(1 + \frac{I_{\mathrm{br}}}{I_{\mathrm{brm}}}\right) = \frac{1}{2} \left(I_{\mathrm{forw}}\right)_{\mathrm{m}} \left(1 + \frac{I_{\mathrm{br}}}{I_{\mathrm{brm}}}\right) \tag{46}$$

it follows that
$$\boxed{\frac{P}{P_m} = \frac{1}{4}\left(1 + \frac{I_{\mathrm{br}}}{I_{\mathrm{brm}}}\right)^2} \tag{47}$$

There is now a standing wave also on the transmission line to the reference cavity. To know its maximal voltage we again calculate $(1+|\rho|)V_{\mathrm{forw}}$. From (39) and (46), after some algebra (see Appendix B)

$$V_{\max} = \left(1 + |\rho|\right) V_{\mathrm{forw}} = \begin{cases} \left(V_{\mathrm{forw}}\right)_{\mathrm{m}} & \text{when } I_{\mathrm{br}} \le I_{\mathrm{brm}} \\ \dfrac{I_{\mathrm{br}}}{I_{\mathrm{brm}}} \left(V_{\mathrm{forw}}\right)_{\mathrm{m}} & \text{when } I_{\mathrm{br}} > I_{\mathrm{brm}} \end{cases} \tag{48}$$

Evidently, to avoid increased voltage, coupling has to be correct for the *highest* expected beam current.

6.2.3 Beam current changes and coupling errors combined

Finally, applying P to the second cavity (which has $Q \neq Q_{\mathrm{m}}$) we have the forward current (more details in appendix C):

$$I_{\mathrm{forw}} = \frac{\sqrt{2P}}{\sqrt{Z}} = \sqrt{\frac{P_m}{2Z}} \left(1 + \frac{I_{\mathrm{br}}}{I_{\mathrm{brm}}}\right) = \frac{1}{2} I_{\mathrm{brm}} \sqrt{\frac{Z_m}{Z}} \left(1 + \frac{I_{\mathrm{br}}}{I_{\mathrm{brm}}}\right) \tag{49}$$

and
$$V_{\mathrm{forw}} = I_{\mathrm{forw}} Z \frac{Z_m}{Z_m} = \frac{1}{2} V_m \sqrt{\frac{Z}{Z_m}} \left(1 + \frac{I_{\mathrm{br}}}{I_{\mathrm{brm}}}\right) \tag{50}$$

Substituting (49) and (50) into (38) we obtain the generalised form of (43):

$$\boxed{\frac{\mathrm{V}}{V_m} = \sqrt{\frac{Q}{Q_m}} \left\{ \left(1 + \frac{I_{\mathrm{br}}}{I_{\mathrm{brm}}}\right) - \frac{I_{\mathrm{br}}}{I_{\mathrm{brm}}} \sqrt{\frac{Q}{Q_m}} \right\}} \tag{51}$$

Note, that as a consequence of equation (51), for $I_{br} < I_{brm}$ and undercoupling ($Q > Q_m$) the cavity field becomes *higher than the nominal one*. This is illustrated in Fig. 26 below, taking the LEP cavity with its nominal gradient of 6 MV/m as example. The used range of Q/Q_m corresponds to what is found in practice for the present fabrication methods of cavities and couplers.

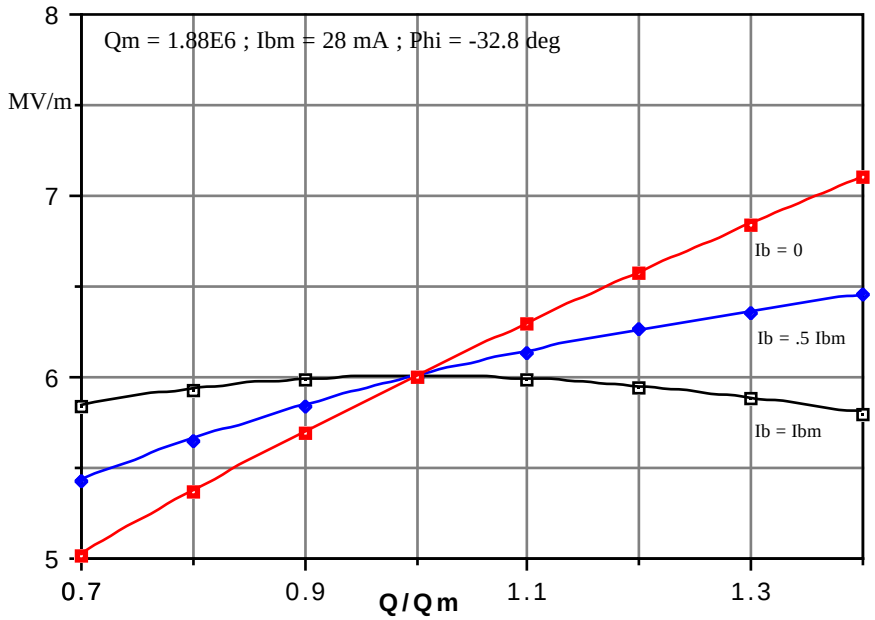

Fig. 26 Coupling dependence of the cavity field for three different beam currents

6.2.4 Tuning errors

All the cavities in an accelerating station have independent tuning loops so, in steady state conditions, tuning errors are insignificant. The situation is different for fast perturbations. Tuner constructions available for sc cavities, since they change the length of the cavity, are rather limited in speed. Even the fastest designs, using magnetostrictive rods, cannot tune out vibrations or beam current changes with frequencies above 10 Hz. It is then necessary to *change the phase* and to *increase the amplitude* of the forward current *to keep the cavity voltage-phasor constant* which, for a calculation of the now required additional forward power, forms the most convenient reference of the phasor diagram in Fig. 27.

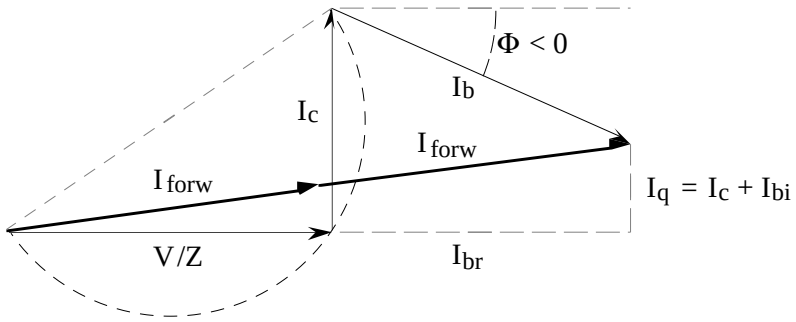

Fig. 27 Same diagram as in Fig. 25, but here V/Z is the reference

Note that here, since we decompose in the direction of V, the values of I_{br} and I_{bi} are different from those in Fig. 25! With $I_q = I_c + I_{bi}$ we now read from the diagram (I_q is a measure of the deviation from correct tuning):

$$\left(2I_{\text{forw}}\right)^2 = \left(\frac{V}{Z} + I_{\text{br}}\right)^2 + \left(I_c + I_{\text{bi}}\right)^2 = \left(\frac{V}{Z} + I_{\text{br}}\right)^2 + {I_q}^2$$

$$\text{it follows} \quad P = \frac{1}{2}\left(I_{\text{forw}}\right)^2 Z = \frac{Z}{8}\left\{\left(\frac{V}{Z} + I_{\text{br}}\right)^2 + {I_q}^2\right\} \tag{52}$$

Evidently, for given cavity voltage, RF beam current and synchronous phase (i.e. beam power) the required forward power P depends on Z (coupling) and I_q (tuning) and to *minimize* P we have to satisfy the two equations:

$$\frac{\partial}{\partial I_q} P\left(Z, I_q\right) = 0 \qquad \text{(i)} \qquad \text{and} \qquad \frac{\partial}{\partial Z} P\left(Z, I_q\right) = 0 \qquad \text{(ii)}$$

$$\text{or} \qquad I_q = I_c + I_{\text{bi}} = 0 \qquad \text{(iii)} \qquad \text{and} \qquad I_q^2 + I_{\text{br}}^2 - \left(\frac{V}{Z}\right)^2 = 0 \qquad \text{(iv)}$$

Satisfying (iii) and (iv) we have a match and the minimum minimorum of the forward power. But with a tuning error, $I_q \neq 0$, we still can obtain a *relative minimum* of the forward power by satisfying only (iv). We find the optimal coupling under such conditions to be *tighter than the matching one:*

$$Z_{\text{opt}} = \left(\frac{R}{Q}\right) Q_{\text{opt}} = \sqrt{\frac{V^2}{I_{\text{br}}^2 + I_q^2}} \quad \leq \quad \frac{V}{I_{\text{br}}} = Z_m \tag{53}$$

We now can imagine two scenarios. In the first we had not foreseen a tuning error and matched at a nominal beam current I_{brm} i.e. we had chosen $Z = V/I_{\text{brm}}$. Substituting this value of Z into Eq. (52) we get:

$$P = \frac{V}{8}\left(I_{\text{brm}} + 2I_{\text{br}} + \frac{I_{\text{br}}^2}{I_{\text{brm}}} + \frac{I_q^2}{I_{\text{brm}}}\right)$$

and normalising by the beam power in matched conditions, $P_{\text{bm}} = 0.5VI_{\text{brm}}$, we obtain a more general form of Eq. (47):

$$\frac{P}{P_{\text{bm}}} = \frac{1}{4}\left\{\left(1 + \frac{I_{\text{br}}}{I_{\text{brm}}}\right)^2 + \left(\frac{I_q}{I_{\text{brm}}}\right)^2\right\} \tag{54}$$

I_q is related to the deviation df from correct detuning. To first order $I_q/I_{\text{brm}} = 2\text{d}f/\Delta f$ where Δf is the loaded 3 dB bandwidth.

Example:

Recently it has been realised [17] that operated at 6 MV/m the LEP cavity suffers from a ponderomotive mechanical oscillation [18]. These oscillations may be suppressed by operating the cavity on its resonance frequency i.e. with $\omega_c = \omega_g$. But then $I_c = 0$ i.e. $I_q = I_{bi}$ and at the nominal beam current I_{bm}:

$$\frac{P}{P_{\text{bm}}} = \frac{1}{4}\left\{(1+1)^2 + \left(\frac{I_{\text{bim}}}{I_{\text{brm}}}\right)^2\right\} = 1 + \frac{1}{4}\text{tg}^2\,\phi \tag{55}$$

Now for P_{bm} = 120 kW and Φ = -32.8° P = 132.5 kW and $(1 + |\rho|)^2 P$ = 225 kW.

In the second scenario we know I_q in advance and choose $Z = Z_{opt}$. For *zero detuning* we have $Z_{opt} = V/I_b$ and the phasor diagram forms an isosceles triangle. Below the LEP example ($\Phi = -32.8°$) is illustrated.

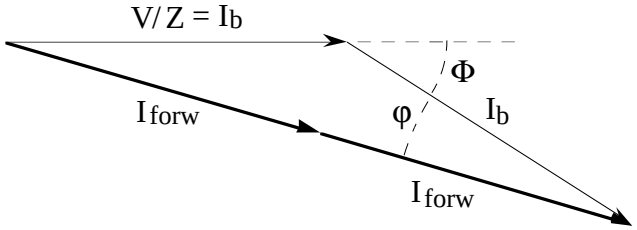

Fig. 28 Phasor sum for zero detuning and optimal coupling

The synchronous phase is now two times the station phase. Substituting Z_{opt} into (52) we find:

$$P = \frac{1}{4} V I_b (1 + \cos\phi) \tag{56}$$

6.2.5 Tuning and coupling errors combined

Finally we will try to visualize what consequences coupling errors have if the cavities of an accelerating station are kept at resonance ($\omega_c = \omega_g$). Here right from the start we had to use a direct numerical approach: First for a reference cavity with $Q = Q_m$ = 1.88E6 and $\Phi = -32.8^\circ$ the station phase φ was determined by solving (36) numerically. Remembering that φ and P are the same for all cavities in a station we then can proceed to determine Φ and P_b for cavities with different *external* Q_s in using (36) and (41). The results are shown in Fig. 29. In contrast to the case of correct tuning the synchronous phase (the phase angle *difference* between cavity voltage and RF beam current) now depends on cavity coupling and rises with increasing *external Q*. Undercoupling thus leads to a sharper increase of power reflection and at the upper limit of the external Q range the equivalent travelling wave power $(1+|\rho|)^2 P$ rises to 280 kW.

6.3 Hardware considerations

Power couplers for sc cavities are normal conducting (nc) devices. Hence their designs could take over many features of earlier constructions for nc cavities. Such couplers may be subdivided into three functional units: first the coupling element proper, probe, loop or coupling iris. Second a ceramic window which seals off the cavity vacuum while letting through the RF power. Third a transition piece to the standard wave guide of the power distribution system.

Couplers for sc cavities have one element more to bridge the gap between room and liquid He temperature while keeping, compared to the cavity dissipation, the heat flux into the He bath small. This thermal transition is a length of guide or line where special care has been taken to minimize both the metal cross-section and thermal conductivity by using copper-plated stainless steel. In addition, cooling with cryogenic gases (He or N_2) is employed to intercept heat at discrete points or continuously in a counter current-flow fashion, very similar to the current leads for sc magnets.

For powers around 100 kW and frequencies around 400 MHz wave guides have unnecessarily large cross-sections. So the coaxial line geometry is the preferred ending, to avoid heat conduction by the inner conductor, in an open circuit as the probe which couples to the electric cavity field within the cut-off tube near to one of the cavity end cells. Thus from the inner conductor only heat radiation can reach the He bath and its operation even at room-temperature becomes feasible if no cold window is employed.

Use of such a second cold window (at ≈ 70 K) was the rule in earlier coupler constructions [19,20]. It was felt that only in this way the sensitive sc surfaces of the cavity could be protected if, under the action of the RF fields, gas molecules would be desorbed from 6warm parts of the coupler and especially from its first room-temperature window.

With the argument that the thermal transition piece should act as an efficient baffle, later [21] only the warm window was kept[4] allowing the use of window constructions with a proven performance from copper-cavity work. Figure 30 shows the LEP power coupler as an example of this approach. Window and 'door-knob' transition to a waveguide are taken over from the coupler for the LEP copper cavities.

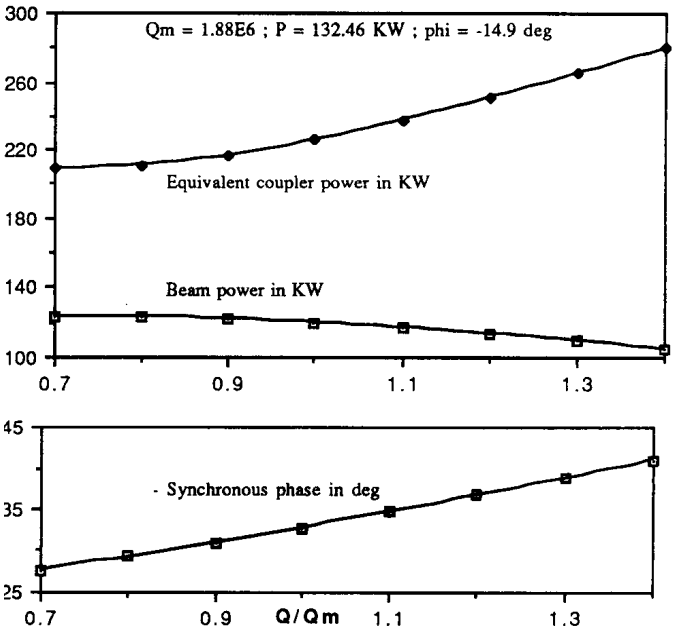

Fig. 29 Influence of coupling errors for LEP cavities operated at resonance

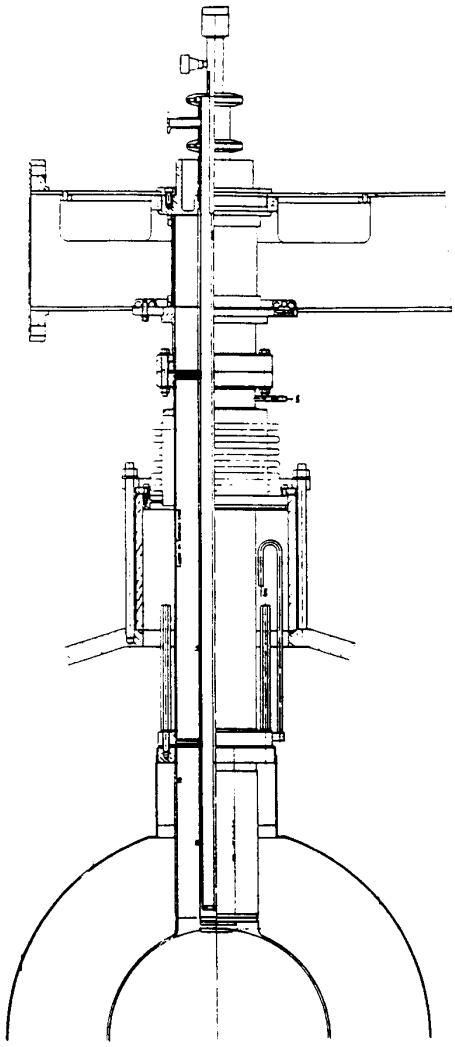

Fig. 30 A LEP power coupler with 50 Ω coaxial line

6.4 Conditioning

Applying for the first time higher powers to vacuum RF devices is often a very delicate operation. In fact, if the power is raised abruptly one risks provoking violent discharges which may destroy the device. Two phenomena combine to create this danger. The first is the

---

[4] The developments for the 1.5 GHz TESLA very-high-gradient sc linac, to be operated at 1.8 K, have reintroduced a second 70 K window as heat shield and to seal the cavity at an early stage of manufacture against dust particle intrusion.

presence of adsorbed layers of gas (predominantly H_2O) molecules on RF boundary surfaces. The second is the existence of electron orbits which, starting and ending on surfaces, become self replicating at certain field levels. If now at such a kinematic "multipactor" resonance an initial electron has an impact energy high enough to release more than one secondary then an avalanche occurs with a proportional increase of gas desorption. If the process is not controlled the local gas pressure may rise to the level where ordinary gas discharges set in.

But gas desorption is not only a danger. It is also the effect which makes *"conditioning"* possible. In fact, the secondary emission coefficient of a copper surface (and similarly for other metals) decreases when H_2O layers are removed [22], so multipactor discharges have the tendency to eliminate themselves. To make a discharge disappear one only has to "tickle" it long enough, taking care that pressure bursts do not rise into the unsafe region above 10^{-7} Torr.

6.5 Deconditioning

Couplers for copper cavities are conditioned together with the cavity. Couplers for sc cavities need more elaborate procedures. Their operation is often plagued by the *reappearance* of multipactor discharges *(deconditioning)*. This is caused by the baffle action of the warm-cold transition [23].

It has been shown that multipactor orbits in coaxial [24] lines with wave impedances bigger than 50 Ω start and end on the outer conductor alone which, acting as a cold trap, is unfortunately also the zone to where molecules liberated in the warm window area are cryopumped. Multipactoring recreated in this way is very difficult to condition. Probably molecules desorbed by electron impact are only partially pumped away, the remainder is re-adsorbed at cold surfaces nearby.

To alleviate the problem of deconditioning, power couplers for sc cavities are, after a thorough bake out at 200°C, *preconditioned* on a separate room-temperature test stand and only then transferred to the cavity. Since, during this last operation, contact with humid air is unavoidable LEP couplers are subsequently baked a second time *in situ*. The window is heated to 200°C for 24 hours. Only then are the cavities cooled and RF power applied for the final conditioning.

As a further safeguard against the reappearance of multipacting the LEP coupler has been fitted with condensers [25] which isolate the central conductor of the coaxial line for DC voltages but let the RF power pass. So, if required, a bias voltage can be applied [26]. It has been found that a bias of 2.5 kV suppresses all multipactor resonances up to a travelling-wave power of at least 200 kW.

Finally, since multipactor resonances belong to certain *E*-field levels at the *outer* conductor, power flow before multipacting sets in will be the higher the *smaller the central conductor's diameter*. With respect to multipacting characteristics the conventional choice of a 50 Ω wave impedance is not optimal. In consequence the LEP power coupler's antenna diameter recently has been reduced from 45 mm to 30 mm which corresponds to $Z_0 = 75\ \Omega$.

REFERENCES

[1] V. Rödel, E. Haebel, The Effect of the Beam Tube Radius on Higher Order Modes in a Pill-Box RF Cavity, SL/RFS/Note 93-17.

[2] V. Rödel, L. Verolino, Geometry of a Superconducting 400 MHz Accelerating Cell for the LHC, SL/RFS/Note 91-11.

[3] W. Hartung, In Search of Trapped Modes in the Single Cell Cavity Prototype for CESR-B, Proc. of the 1993 PAC, Washington, p.898.

[4] E. Haebel and A. Mosnier, Large or Small Iris Aperture in SC Multicell Cavities? Proc. of the 5th Workshop on RF-Superconductivity, DESY, 1991, p. 823.

[5] F. Caspers, Experience with UHV Compatible Microvave Absorbing Materials at CERN, PS 93-10 (AR).

[6] D. Moffat et al., Design and Fabrication of a Ferrite-lined HOM Load for CESR-B, Proc. of the 1993 PAC, Washington, p. 977.

[7] T. Tajima et al., Bonding of a Microwave-Absorbing Ferrite with Copper for the HOM Damper of the KEK B-Factory SC Cavities, KEK Preprint 93-152, November 1993.

[8] T. Tajima et al., Development of HOM Absorber for the KEK B-Factory SC Cavities, Proc. of the 6th Workshop on RF-Superconductivity, CEBAF, 1993, p.962.

[9] E. Plawski, Influence of the Bunch Length on the HOM Power Deposition in the SC LEP Cavities, CERN LEP2 Note 94-19.

[10] W. Schminke, SPS/ARF/WS/gs/81-68,CERN 1981.

[11] E. Haebel, Fundamental and HOM couplers on SC Cavities for Electron Storage Rings, Proc. of the 1983 PAC, Santa Fe, New Mexico, p. 3345.

[12] E. Haebel and J. Sekutowicz, Higher Order Mode Coupler Studies at DESY, DESY-Report M-86-06, July 1986.

[13] J. Sekutowicz, Higher Order Mode Coupler for TESLA, Proc. of the 6th Workshop on RF-Superconductivity, CEBAF, 1993, p. 426.

[14] S. Chel et al., Thermal Tests of HOM Couplers for Superconducting Cavities, Proc. of the 1994 EPAC, p. 2007 .

[15] Ph. Bernard et al., Demountable E/H-Field HOM Couplers for the Niobium Sputtered LEP Cavity, Proc. of the 5th Workshop on RF-Superconductivity, DESY, 1991, p. 956.

[16] P.B. Wilson, High Energy Electron Linacs: Application to Storage Ring RF Systems and Linear Colliders, SLAC-PUB-2884, Feb. 1982.

[17] D. Boussard et al., Electroacoustic Instabilities in the LEP2 Superconducting Cavities, Proc. of the 7th Workshop on RF-Superconductivity, Gif sur Yvette, 1995.

[18] M.M. Karliner et al., Instability in the Walls of a Cavity due to Ponderomotive Forces of the Electromagn. Field, Soviet Physics-Technical Physics, Vol. 11, No 11, May 67.

[19] A. Citron et al. and H. Lengeler, The Karlsruhe-CERN Superconducting RF Seperator, Nucl. Instr. Meth. 164 (1979) p. 31.

[20] L. Szeczi and R. Lehm, Theor. und Techn. Beschr. eines 100 KW Koppelsystems für einen supraleitenden Beschleunigungsresonator, Primärbericht 9/81, KFK, Karlsruhe.

[21] E. Haebel, Beam tube Couplers for the Superconducting LEP Cavity,, Proc. of the 2nd Workshop on RF-Superconductivity, CERN, 1984, p. 299.

[22] J. Barnard et al., Secondary Electron Emission from Various Technical Materials and Condensed Gases, Proc. of the 7th Workshop on RF-Superconductivity, Gif sur Yvette, 1995.

[23] E. Haebel et al., Gas Condensation on Cold SuRFaces, a Source of Multipacting Discharges in the LEP Power Coupler, Proc. of the 7th Workshop on RF-Superconductivity, Gif sur Yvette, 1995.

[24] E. Somersalo et al., Analysis of Multipacting in Coaxial Lines, Proc. of the 1995 PAC, Dallas, Texas.

[25] H.P. Kindermann et al., Status of the RF Power Couplers for Superconducting Cavities at CERN, to be Published in Proc. of the 1996 EPAC, Sitges (Barcelona).

[26] J. Tückmantel et al., Improvements to Power Couplers for the LEP2 Superconducting Cavities, Proc. of the 1995 PAC, Dallas, Texas.

APPENDIX A

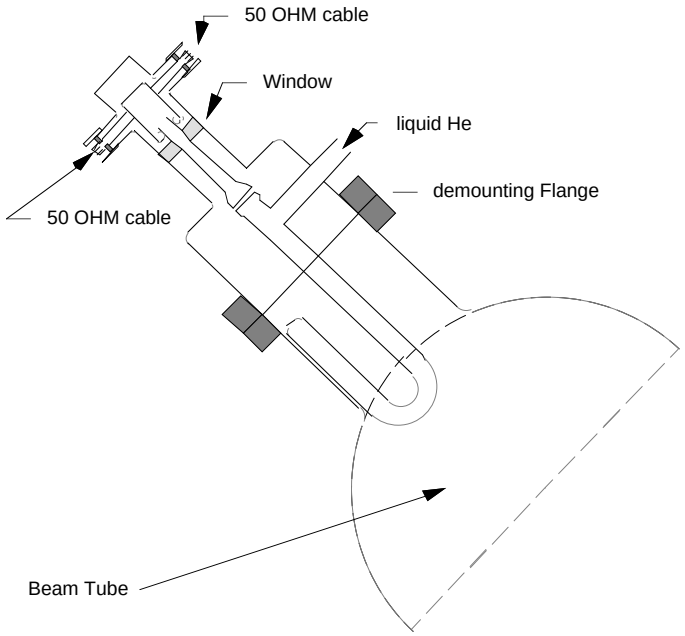

Fig. 1 Geometry of the HOM coupler used in LEP

Table 1
Damping of significant HOM with two couplers per LEP cavity

f/MHz	461	476	506	513	639	688	1006
Mode	TE_{111}	TE_{111}	TM_{110}	TM_{011}	TM_{111}	TM_{111}	TM_{012}
$(R/Q)/\Omega$	18	15	20	13	56	25	16
Q_{ex}	17 000	14 000	5600	5700	7000	1000	2000

APPENDIX B

From

$$V = I_{\text{forw}}\, Z_m \left(2 - \frac{I_{\text{br}}}{I_{\text{forw}}} \right) \equiv V_m = I_{\text{brm}}\, Z_m \tag{B1}$$

we obtain

$$2 I_{\text{forw}} = I_{\text{brm}} + I_{\text{br}} \tag{B2}$$

and using Eq. (39) from the main body of this lecture

$$\text{we have} \qquad \rho = 1 - \frac{I_{br}}{I_{forw}} = \frac{2I_{forw} - 2I_{br}}{2I_{forw}} = \frac{I_{brm} - I_{br}}{I_{brm} + I_{br}} \tag{B3}$$

and remembering that $I_{brm} = (I_{forw})_m$ we get

$$1 + |\rho| = \begin{cases} \dfrac{2I_{brm}}{I_{brm} + I_{br}} = \dfrac{(I_{forw})_m}{I_{forw}} = \dfrac{(V_{forw})_m}{V_{forw}} & \text{when } I_{br} \le I_{brm} \\ \dfrac{2I_{br}}{I_{brm} + I_{br}} = \dfrac{I_{br}}{I_{brm}} \dfrac{(V_{forw})_m}{V_{forw}} & \text{when } I_{br} > I_{brm} \end{cases} \tag{B4}$$

$$\text{and} \quad V_{max} = (1 + |\rho|) V_{forw} = \begin{cases} (V_{forw})_m & \text{when } I_{br} \le I_{brm} \\ \dfrac{I_{br}}{I_{brm}} (V_{forw})_m & \text{when } I_{br} > I_{brm} \end{cases} \tag{B5}$$

APPENDIX C

From the main body of the lecture:

$$V = V_{forw}\left(2 - \frac{I_{br}}{I_{forw}}\right) \tag{C1}$$

$$\text{and} \qquad \sqrt{\frac{P_m}{2Z}} = \frac{\sqrt{2P_m}}{2\sqrt{Z}} = \frac{(I_{forw})_m \sqrt{Z_m}}{2\sqrt{Z}} = \frac{1}{2} I_{brm} \sqrt{\frac{Z_m}{Z}} \tag{C2}$$

$$\text{and} \qquad I_{forw} = \frac{\sqrt{2P}}{\sqrt{Z}} = \sqrt{\frac{P_m}{2Z}}\left(1 + \frac{I_{br}}{I_{brm}}\right) \tag{C3}$$

$$\text{it follows that} \qquad I_{forw} = \frac{1}{2} I_{brm} \sqrt{\frac{Z_m}{Z}}\left(1 + \frac{I_{br}}{I_{brm}}\right) \tag{C4}$$

$$\text{and} \qquad V_{forw} = I_{forw} Z \frac{Z_m}{Z_m} = \frac{1}{2} V_m \sqrt{\frac{Z}{Z_m}}\left(1 + \frac{I_{br}}{I_{brm}}\right) \tag{C5}$$

substituting (C4) and (C5) into (C1):

$$\frac{V}{V_m} = \sqrt{\frac{Z}{Z_m}}\left[\left(1 + \frac{I_{br}}{I_{brm}}\right) - \frac{I_{br}}{I_{brm}} \sqrt{\frac{Z}{Z_m}}\right] \tag{C6}$$